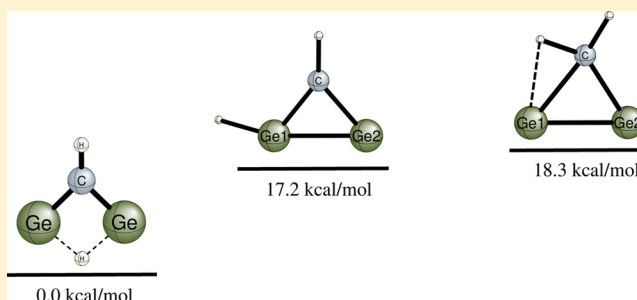


Structures and Transition States of Ge_2CH_2 Stefan Vogt-Geisse, Alexander Yu. Sokolov, Shane R. McNew, Yukio Yamaguchi,
and Henry F. Schaefer III*

Center for Computational Quantum Chemistry, University of Georgia, Athens, Georgia 30602, United States

Supporting Information

ABSTRACT: In this study a systematic theoretical investigation of Ge_2CH_2 is carried out. The singlet potential energy surface (PES) was explored using state-of-the-art theoretical methods including self-consistent field (SCF), coupled cluster theory incorporating single and double excitation (CCSD), perturbative triple [CCSD(T)] and full triples [CCSDT] with perturbative quadruple (Q), together with a variety of correlation-consistent polarized valence basis sets cc-pVXZ (where X = D, T, and Q). A total of eleven stationary points have been located on the Ge_2CH_2 singlet ground state PES. Among them, seven structures are minima (1S–7S), two are transition states (TS1 and TS2), and two are second-order saddle points (SSP1 and SSP2). The global minimum is predicted to be an exotic hydrogen-bridged structure 1S. The energy ordering of the seven minima (in kcal mol^{−1}) obtained from focal point analysis using the extrapolation to complete basis set (CBS) limit with zero point vibrational energy (ZPVE), core correlation, diagonal Born–Oppenheimer (DBOC) and relativistic correction is 1S [0.0] < 2S [17.2] < 3S [18.3] < 4S [31.7] < 5S [39.9] < 6S [58.1] < 7S [82.1].



I. INTRODUCTION

The chemistry of germanium is rapidly developing. It is now widely realized that germanium atoms can form stable compounds in the divalent (carbene-like) as well as the expected tetravalent state and exhibits a variety of binding motifs.¹ Species with multiple bonds to germanium have been reported.^{1–3} Furthermore, germanium has been shown to form strained three- and four-membered rings,^{1,2} including aromatic molecules with two and six π -electrons.^{4–7}

Among the simplest divalent species, germanium containing compounds $\text{Ge}_n\text{C}_{3-n}\text{H}_2$ ($n = 1–3$) are of particular interest.⁸ These molecules are valence isoelectronic to cyclopropenylidene (C_3H_2) and its silicon derivatives (SiC_2H_2 and Si_2CH_2), which have drawn much attention due to their unique reactivity and primal role in the chemistry of the interstellar medium.^{9,10} Several experimental and theoretical studies have been carried out to determine the structures of the C_3H_2 isomers^{11–19} and its silicon analogues.^{20–32} The two lowest-energy structures located on the singlet potential energy surface (PES) of C_3H_2 are the cyclic isomer $:\text{C}(\text{CH})_2$ and the propadienylidene structure $:\text{C}=\text{C}=\text{CH}_2$ ¹⁷ (Figure 1). The lowest energy triplet structure of C_3H_2 was found to lie close in energy to propadienylidene.¹⁹ Interestingly, the ground state of C_3H_2 is isoelectronic to the deprotonated cyclopropenium ion $[\text{C}_3\text{H}_3]^+$ with two π -electrons and can therefore be considered the smallest aromatic carbene.

In 1986 Frenking et al.²⁰ investigated structural isomers of SiC_2H_2 at the Hartree–Fock (HF) and the configuration interaction with singles and double excitations (CISD) levels of theory. They found that singlet 1-silacyclopentenylidene

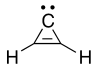
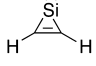
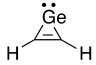
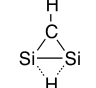
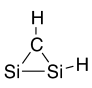
Compound	Global Minimum	Second Lowest
C_3H_2	 (0.0)	$\text{H}-\text{C}=\text{C}=\text{C}:$ (13.3)
SiC_2H_2	 (0.0)	$\text{H}-\text{C}=\text{C}=\text{Si}:$ (17.6)
GeC_2H_2	 (0.0)	$\text{H}-\text{C}=\text{C}=\text{Ge}:$ (13.5)
Si_2CH_2	 (0.0)	 (14.5)

Figure 1. Two lowest energy isomers of XC_2H_2 ($\text{X} = \text{C}, \text{Si}, \text{Ge}$) and Si_2CH_2 . The theoretical energies (in kcal mol^{−1}) relative to the corresponding global minimum structures are given in parentheses. The relative energies are taken from refs 19 (C_3H_2), 28 (SiC_2H_2), 34 (GeC_2H_2), and 31 (Si_2CH_2).

($:\text{Si}(\text{CH})_2$) was the lowest energy structure (Figure 1). Matrix isolation infrared (IR) spectroscopy experiments performed by Maier and co-workers^{21–23} detected four different isomers of SiC_2H_2 . The cyclic $:\text{Si}(\text{CH})_2$ was confirmed to be the global minimum of the SiC_2H_2 system. More recent high accuracy *ab initio* studies employing the coupled cluster (CC) theory methods supported the previous experimental and theoretical

Received: March 8, 2013

Revised: June 5, 2013

Published: June 17, 2013

results about the energetic ordering of various SiC_2H_2 isomers.^{24–28} The geometric and electronic structure of Si_2CH_2 is fundamentally different from those of C_3H_2 and SiC_2H_2 . The SiC_2H_2 system was first studied by Jemmis et al.²⁹ using the second order Møller–Plesset (MP2) method. Jemmis found an unusual hydrogen-bridged cyclic structure $(\text{Si}\cdots\text{H}\cdots\text{Si})(\text{CH})$ with three-center two-electron $\text{Si}\cdots\text{H}\cdots\text{Si}$ bond to have the lowest energy (Figure 1). This peculiar result was confirmed by the latest studies employing CC theory and the focal point extrapolation technique.^{30,31} Recently, the paper by Lu and co-workers presented an anharmonic rovibrational analysis of the global minimum structure of Si_2CH_2 .³²

The isovalent germanium species $\text{Ge}_n\text{C}_{3-n}\text{H}_2$ ($n = 1–3$) have been investigated to a much lesser extent than the corresponding silicon compounds. The $\text{Ge}(\text{C}_2\text{H}_2)$ complex was produced by laser ablation and detected by matrix isolation IR spectroscopy.³³ Two structural isomers were characterized: cyclic germylene $:\text{Ge}(\text{CH})_2$ isomer (1-germacyclopropenyli-dene, Figure 1) and bent ethynylgermylene. The magnitude of the C–C stretching vibrational frequency in the cyclic isomer indicated that its structure is similar to that of C_3H_2 , as opposed to the metal–acetylene π -complex. A very recent theoretical study of GeC_2H_2 structures and energetics using the coupled cluster methods located a total of nine different structural isomers on the singlet PES at the CCSD(T)/cc-pV(Q+d)Z level of theory. The cyclic $:\text{Ge}(\text{CH})_2$ isomer was found to be the global minimum (in Figure 1).³⁴ The computed C–C stretching harmonic vibrational frequency of the cyclic isomer was found to be in very good agreement with the experiment.³³

To our knowledge, no reports have been found about the Ge_2CH_2 species in the literature. In this research, using highly reliable coupled cluster methods we predict geometric structures, relative energies, harmonic vibrational frequencies, and associated infrared (IR) intensities of various Ge_2CH_2 isomers. A total of eleven stationary points were located on the Ge_2CH_2 PES. Among these there are two isomers with very unusual bonding patterns: **1S** is a hydrogen-bridged structure, and **3S** possesses a peculiar tetravalent planar carbon.

II. THEORETICAL PROCEDURES

A stochastic search using the kick procedure developed by Saunders^{35–37} was utilized, in order to systematically search for stationary points on the singlet potential energy surface (PES). The initial geometries for optimization were generated by randomly displacing the atoms from a starting position in which all atoms fall on the same point in space. For the sake of minimizing computational effort three conditions were applied, during the stochastic search: (1) No atom could be kicked farther than 4.5 Å from its initial position, (2) the minimal distance between any two atoms has to be greater than 1.0 Å, and (3) the maximal distance between any two atoms should not be greater than 6.0 Å. Five hundred structures that met these requirements were generated. Subsequently these structures were optimized using the B3LYP method with a 6-31G basis set. Of the 500 structures the optimization procedure was successful in 154 cases which were distributed among 7 minima on the PES. Optimizations were done using the QCHEM quantum chemistry software package.³⁸

The optimization was refined using the correlation-consistent polarized valence basis sets cc-pVXZ ($X = \text{D}, \text{T}, \text{and Q}$) developed by Dunning and co-workers.³⁹ Zeroth-order descriptions of all stationary points were obtained using the

closed-shell restricted Hartree–Fock (RHF) self-consistent field (SCF) method. Dynamic correlation effects were included using the coupled cluster (CC) with single and double excitations (CCSD),^{40,41} CCSD with perturbative triple [CCSD(T)],^{42–44} full triples (CCSDT), and perturbative quadruples [CCSDT(Q)]^{45,46} method. The total of 19 lowest lying core orbitals corresponding to atomic orbitals (AO) 1s, 2s, 2p, 3s, and 3p of germanium and the 1s-like orbital of carbon were kept frozen in the correlated wavefunctions. Due to a relative small energy separation between the 3d and 4s and 4p orbitals (compared to the separation between the 3d and 3s and 3p orbitals), the 3d electrons are included on the correlated procedures.⁴⁷

The nature of the molecular wavefunction of each stationary point was analyzed using the complete active space self-consistent field method (CASSCF)^{48,49} with the cc-pVQZ basis set at the CCSD(T)/cc-pVQZ optimized geometries. The active space was chosen to be 10 electrons in 9 molecular orbitals (MOs). For the representation of the CASSCF wavefunctions the reduced one-particle density matrix was diagonalized to obtain the natural orbitals and occupation numbers.⁵⁰

The relative energies of eleven different Ge_2CH_2 stationary points with respect to the global minimum (**1S**) were obtained using the focal point analysis technique (FPA).^{51–54} In this technique, energy values obtained at the SCF, MP2, CCSD, CCSD(T), (CCSDT), and CCSDT(Q) levels of theory with the cc-pVXZ basis sets were used to obtain relative energies extrapolated to the complete basis set (CBS) limit. The geometries employed in the focal point analysis (FPA) were optimized at the CCSD(T)/cc-pVQZ level of theory. In the FPA procedure the total energy was extrapolated to the complete basis set limit (CBS) using the functional form^{55,56}

$$E_{\text{SCF}}(X) = A + (B e^{-CX})$$

$$E_{\text{CORR}} = E + FX^{-3}$$

where E_{SCF} and E_{CORR} are the extrapolated SCF and correlation energies, and X is the cardinal number corresponding to the maximum angular momentum of the basis set. A , B , C and E , F are fitting parameters for the SCF and correlation energies, respectively.

Core correlation (ΔE_{core}) effects were computed as the difference between frozen-core and all-electron CCSD(T)/cc-pCVQZ energies using the MOLPRO.⁵⁷ Energy contributions beyond the Born–Oppenheimer approximation (ΔE_{DBOC}) have been included via the diagonal Born–Oppenheimer correction (DBOC), at the CCSD/cc-pVTZ level of theory.⁵⁸ Finally, special relativity effects (ΔE_{rel}) were accounted for by the application of the mass-velocity and Darwin one-electron terms⁵⁹ computed at CCSD(T)/cc-pVQZ level of theory. Both corrections were computed with the CFOUR software package.⁶⁰ The structures of the Ge_2CH_2 isomers were optimized using analytic derivative methods. Harmonic vibrational frequencies were also determined analytically. The harmonic vibrational frequencies were used to characterize the nature of each stationary point on the Ge_2CH_2 PES. The reported IR intensities were obtained via the double harmonic (mechanical and electronic) approximation. Electronic structure computations were carried out using CFOUR⁶⁰ and MOLPRO⁵⁷ quantum chemistry software packages.

III. RESULTS AND DISCUSSION

Figures 2 to 6 show the optimized structures of eleven stationary points located on the Ge_2CH_2 singlet ground state PES at the CCSD(T)/cc-pVQZ level of theory. Among these, seven structures are minima (**1S**–**7S**), two are transition states (**TS1** and **TS2**), and two are stationary points of Hessian index 2 (**SSP1** and **SSP2**). Three lowest energy structures **1S**–**3S** are cyclic (shown in Figures 2 to 4). Structures **4S**–**6S** are open-chain with linear (**4S** and **5S**) and bent (**6S**) $\{\text{Ge}_2\text{C}\}$ fragments (shown in Figure 5). Focal point analyses (FPA) of the relative energies between isomers **1S**, **2S**, and **3S** are provided in Table 1 and Table 2, respectively. For the remaining stationary points the relative energies from FPA are given in Tables S1–S8 (Supporting Information). The final energies (with the ZPVE, core, DBOC, and relativistic corrections) for the eleven stationary points located on the singlet PES are presented in Table 3. The triplet states of the low-energy structures are more than 30 kcal mol^{−1} higher in energy than the corresponding singlet states and, therefore, will not be discussed in this paper.

A. Relative Energies and CASSCF Wavefunctions.

The nature of the molecular wavefunctions was analyzed using the CASSCF method with the cc-pVQZ basis set. For each of the stationary points the wavefunction has a dominant contribution from a single electronic (reference) configuration. The single reference nature of the system was confirmed via the T1 and T2 diagnostic at the CCSD(T)/cc-pVQZ level of theory (Table S17 in the Supporting Information). The values of the T1 and T2 amplitudes lie below the multireference threshold.

i. Global Minimum 1S. The ground electronic configuration for the unconventional C_{2v} symmetry global minimum structure **1S** (in Figure 2) is mainly described as

$$\Phi_1 = [\text{core}]12a_1^2 13a_1^2 11b_2^2 14a_1^2 15a_1^2 12b_2^2 5b_1^2$$

$$|\text{CI}|^2 = 0.90$$

where [core] denotes the 29 low-lying doubly occupied MOs (including the 3d orbitals of Ge) and $|\text{CI}|^2$ is the square of the corresponding configuration interaction (CI) coefficient. The next two doubly excited configuration state functions (CSFs) are $\Phi_2[5b_1^2 \rightarrow 6b_1^2]$ ($|\text{CI}|^2 = 0.01$) and $\Phi_3[5b_1^2 \rightarrow 5a_1^2]$ ($|\text{CI}|^2$

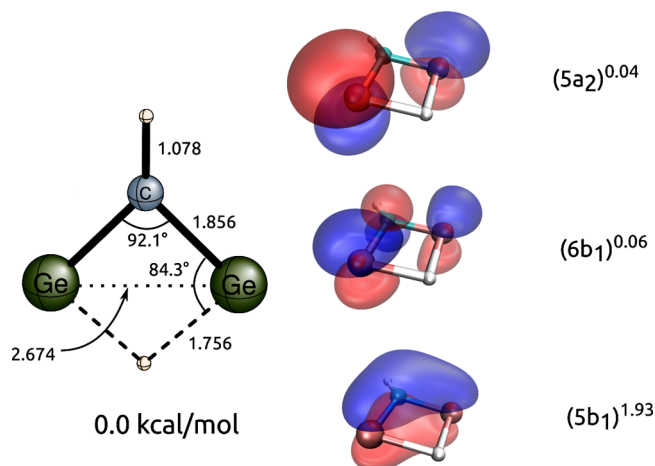


Figure 2. Geometry of the Ge_2CH_2 global minimum structure **1S** (C_{2v} symmetry) optimized at the CCSD(T)/cc-pVQZ level of theory (on the left). Plots of its CASSCF frontier natural orbitals are shown on the right. The symmetries and the occupancies of three relevant natural orbitals are also shown.

< 0.01). As one can see in Figure 2, these excitations correspond to the electronic transitions from the bonding π -type $5b_1$ orbital to the antibonding π^* -type $6b_1$ ($\pi \rightarrow \pi^*$ transition) and nonbonding $5a_2$ orbitals. The heat of formation at 0 K for the global minimum was computed using the reaction $2\text{GeH}_4 + \text{CH}_4 \rightarrow \text{Ge}_2\text{CH}_2 + 5\text{H}_2$. The reaction energy was computed at the CCSD(T)/cc-pVTZ level of theory, and the experimental heats of formation for gas phase GeH_4 and CH_4 were obtained from ref 61. The heat of formation for **1S** was found to be 129.2 kcal mol^{−1}

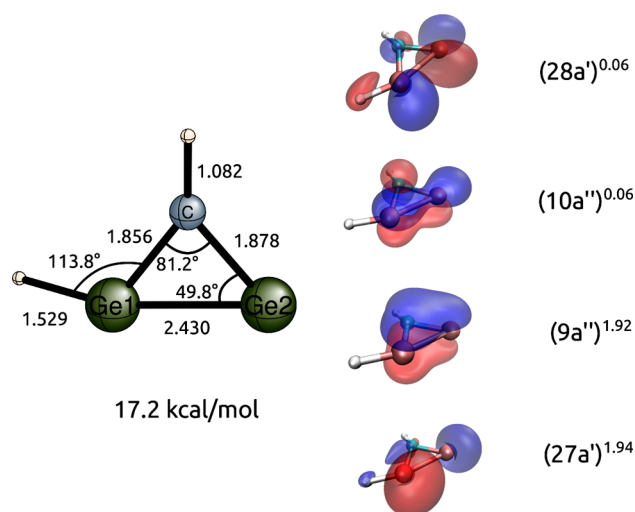


Figure 3. Geometry of the Ge_2CH_2 isomer **2S** (C_s symmetry) optimized at the CCSD(T)/cc-pVQZ level of theory (on the left). Plots of its CASSCF frontier natural orbitals are shown on the right. The energy relative to the global minimum **1S** is computed at the CCSDT(Q)/CBS level of theory. The symmetries and the occupancies of four relevant natural orbitals are also shown.

ii. Structures 2S and 3S (Figures 3 and 4 and Tables 1 and 2). The ground electronic configuration for structures **2S** and **3S** (C_s symmetry, in Figures 3 and 4) is

$$\Phi_1 = [\text{core}]22a'^2 23a'^2 24a'^2 25a'^2 26a'^2 9a''^2 27a'^2$$

$$|\text{CI}|^2 = 0.90(\text{2S}) \text{ and } 0.89(\text{3S})$$

The other two important CSFs are $\Phi_2[9a''^2 \rightarrow 10a''^2]$ [$|\text{CI}|^2 = 0.01$ (**2S**), 0.03 (**3S**)] and $\Phi_3[27a'^2 \rightarrow 28a'^2]$ [$|\text{CI}|^2 < 0.01$ (**2S**, **3S**)]. The former CSF corresponds to the $\pi \rightarrow \pi^*$ transition, whereas the latter describes a transition within the in-plane σ -orbital framework, as shown in Figures 3 and 4.

As may be seen from Table 1, the **2S** isomer is found to lie 17.7 kcal mol^{−1} (without four corrections) higher in energy than the global minimum **1S**. At the SCF/cc-pVQZ level of theory the energy difference between these two isomers is 18.3 kcal mol^{−1}, which is only 0.5 kcal mol^{−1} higher than the energy obtained at the CCSDT(Q)/CBS, showing that the inclusion of correlation treatment has only little effect on this particular energy difference.

The focal point analysis (FPA) for the energy difference between isomers **1S** and **3S** is presented in Table 2. The energy separation is predicted to be 18.0 kcal mol^{−1} (without four corrections). The inclusion of correlation effects seem to play a more preponderant role for the **3S** since it decreases the energy from 21.9 kcal mol^{−1} at the SCF/CBS level to 18.0 kcal mol^{−1}

Table 1. Focal Point Analysis of the Relative Energy between Isomers 1S and 2S (ΔE_{final} , kcal mol⁻¹)^a

	$\Delta E_e[\text{RHF}]$	+ δMP2	+ δCCSD	+ $\delta\text{CCSD(T)}$	+ δCCSDT	+ $\delta\text{CCSDT(Q)}$	NET
cc-pVDZ	+18.05	+1.59	-0.29	+0.01	-0.06	-0.03	[+19.26]
cc-pVTZ	+18.22	+0.91	-0.38	+0.05	[-0.06]	[-0.03]	[+18.71]
cc-pVQZ	+18.25	+0.39	-0.41	+0.04	[-0.06]	[-0.03]	[+18.18]
cc-pVSZ	+18.27	+0.16	[-0.41]	[+0.04]	[-0.06]	[-0.03]	[+17.96]
CBS LIMIT	[+18.27]	[-0.09]	[-0.41]	[+0.04]	[-0.06]	[-0.03]	[+17.72]
$\Delta E_{\text{final}} = \Delta E_e[\text{CCSDT(Q)/CBS}] + \Delta_{\text{ZPVE}}[\text{CCSD(T)/cc-pVQZ}] + \Delta_{\text{CORE}}[\text{CCSD(T)/cc-pCVQZ}] + \Delta_{\text{DBOC}}[\text{CCSD/cc-pVTZ}] + \Delta_{\text{rel}}[\text{CCSD/cc-pVTZ}] = +17.72 - 0.40 - 0.09 - 0.00 - 0.00 = 17.23 \text{ kcal mol}^{-1}$							

^aThe symbol δ denotes the increment in the relative energy (ΔE_e) with respect to the preceding level of theory in the hierarchy SCF \rightarrow MP2 \rightarrow CCSD \rightarrow CCSD(T) \rightarrow CCSDT \rightarrow CCSDT(Q). Square brackets signify results obtained from basis set extrapolations or additivity assumptions. Final extrapolated values are boldfaced.

Table 2. Focal Point Analysis of the 3S Isomer Relative Energy between Isomers 1S and 3S of (ΔE_{final} , kcal mol⁻¹)^a

	$\Delta E_e[\text{RHF}]$	+ δMP2	+ δCCSD	+ $\delta\text{CCSD(T)}$	+ δCCSDT	+ $\delta\text{CCSDT(Q)}$	NET
cc-pVDZ	+21.98	-3.30	+0.77	-0.65	+0.07	-0.13	[+18.74]
cc-pVTZ	+21.73	-3.21	+1.14	-0.82	[+0.07]	[-0.13]	[+18.78]
cc-pVQZ	+21.92	-3.97	+1.47	-0.89	[+0.07]	[-0.13]	[+18.46]
cc-pVSZ	+21.89	-4.16	[+1.47]	[-0.89]	[+0.07]	[-0.13]	[+18.25]
CBS LIMIT	[+21.88]	[-4.36]	[+1.47]	[-0.89]	[+0.07]	[-0.13]	[+18.03]
$\Delta E_{\text{final}} = \Delta E_e[\text{CCSDT(Q)/CBS}] + \Delta_{\text{ZPVE}}[\text{CCSD(T)/cc-pVQZ}] + \Delta_{\text{CORE}}[\text{CCSD(T)/cc-pCVQZ}] + \Delta_{\text{DBOC}}[\text{CCSD(T)/cc-pVQZ}] + \Delta_{\text{rel}}[\text{CCSD(T)/cc-pVQZ}] = +18.03 + 0.63 - 0.38 + 0.02 + 0.01 = 18.31 \text{ kcal mol}^{-1}$							

^aThe symbol δ denotes the increment in the relative energy (ΔE_e) with respect to the preceding level of theory in the hierarchy SCF \rightarrow MP2 \rightarrow CCSD \rightarrow CCSD(T) \rightarrow CCSDT \rightarrow CCSDT(Q). Square brackets signify results obtained from basis set extrapolations or additivity assumptions. Final extrapolated values are boldfaced.

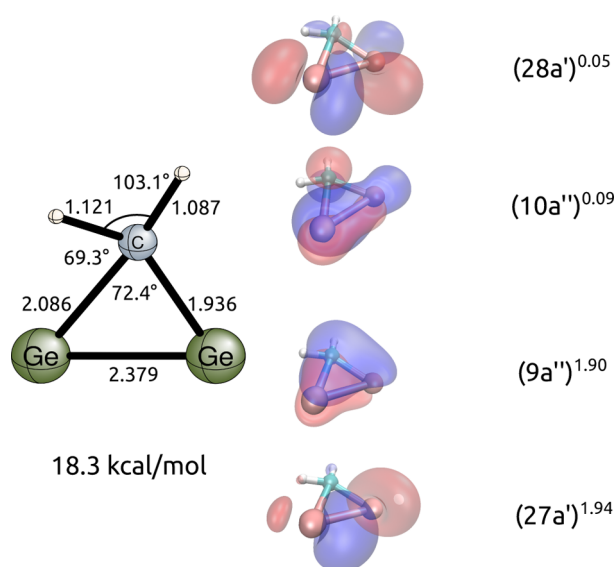


Figure 4. Geometry of the GeC_2H_2 isomer 3S (C_s symmetry) optimized at the CCSD(T)/cc-pVQZ level of theory (on the left). Plots of the CASSCF frontier natural orbitals are shown on the right. The energy relative to the global minimum 1S is computed at the CCSDT(Q)/CBS level of theory. The symmetries and the occupancies of four relevant natural orbitals are also shown.

for the final extrapolated result. This can also be appreciated when looking at the MP2 energy contribution $\delta(\text{MP2})$ increments in Tables 1 and 2. While the MP2 correction to the relative energy at CBS is minimal ($-0.09 \text{ kcal mol}^{-1}$) for the 2S isomer, for 3S, the same quantity amounts to $-4.36 \text{ kcal mol}^{-1}$. The same trend holds using higher level correlated methods [CCSD, CCSD(T)], meaning that correlation effects are more significant for 3S than in the 2S isomer. The total correction from correlation energy in the 3S isomer amounts to $3.85 \text{ kcal mol}^{-1}$, while in 2S it is only $0.55 \text{ kcal mol}^{-1}$. After

including the ZPVE, DBOC, core, and relativistic corrections the energy difference between 1S and 2S becomes $17.2 \text{ kcal mol}^{-1}$. The energy gap between 1S and 3S is $18.3 \text{ kcal mol}^{-1}$.

iii. Structures 4S and 5S (Figure 5 and Tables S1 and S2 in the Supporting Information). The wavefunctions of the noncyclic symmetry isomers 4S and 5S (in Figure 5) are dominated by the following CSFs:

$$\Phi_1 = [\text{core}]16a_1^2 17a_1^2 7b_2^2 18a_1^2 19a_1^2 7b_1^2 8b_2^2$$

$$|\text{CI}|^2 = 0.85 \text{ (4S) and } 0.92 \text{ (5S)}$$

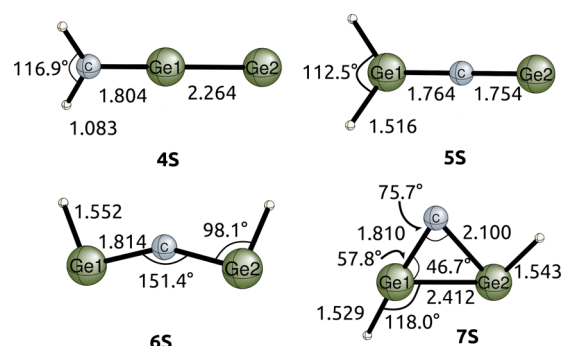


Figure 5. Geometries of the isomers 4S–7S optimized at the CCSD(T)/cc-pVQZ level of theory.

The other two CSFs with significant contributions are $\Phi_2[8b_2^2 \rightarrow 9b_2^2]$ ($|\text{CI}|^2 = 0.05$ for 4S and $|\text{CI}|^2 = 0.02$ for 5S) and $\Phi_3[7b_1^2 \rightarrow 8b_1^2]$ ($|\text{CI}|^2 = 0.03$ for 4S and $|\text{CI}|^2 = 0.01$ for 5S). These excitations correspond to $\pi \rightarrow \pi^*$ transitions in and out of the molecular plane, respectively. The final relative energies of 4S and 5S with respect to the global minimum are 31.7 and $39.9 \text{ kcal mol}^{-1}$ (Table 3).

iv. Structure 6S (Figure 5 and Table S3 in the Supporting Information). The CASSCF wavefunction for the 6S isomer

Table 3. The FPA Extrapolated and Final Corrected Energies (in kcal mol⁻¹) for the Eleven Stationary Points Located on the Singlet Ge₂CH₂ Potential Energy Surface

structure	ΔE_{FPA}	ΔE_{final}
1S	0.00	0.00
2S	17.72	17.23
3S	18.03	18.31
4S	30.88	31.69
5S	40.50	39.89
6S	61.02	58.05
7S	84.80	82.11
TS1	18.33	18.11
TS2	87.85	88.27
SSP1	24.34	22.57
SSP2	105.69	103.73

(Figure 5) with bent {Ge–C–Ge} fragment (*C*_{2v} symmetry) has a dominant contribution from the following CSF:

$$\Phi_1 = [\text{core}]12a_1^2 11b_1^2 13a_1^2 12b_2^2 14a_1^2 5b_1^2 13b_2^2$$

$$|\text{CI}|^2 = 0.85$$

The next two dominant excitations, $\Phi_2[14a_1^2 \rightarrow 15a_1^2]$ ($|\text{CI}|^2 = 0.01$) and $\Phi_3[5b_1^2 \rightarrow 6b_1^2]$ ($|\text{CI}|^2 = 0.01$), correspond to transitions within the σ - and π -orbital framework of the {Ge–C–Ge} fragment, respectively. The final energy separation between 1S and 6S is 58.1 kcal mol⁻¹ (Table 3).

v. *Structure 7S* (Figure 5 and Table S4 in the Supporting Information). The electronic state of the 7S structure (*C*_s symmetry, in Figure 5) is mainly described by the configuration

$$\Phi_1 = [\text{core}]22a^2 23a^2 24a^2 25a^2 26a^2 9a^2 27a^2$$

$$|\text{CI}|^2 = 0.86$$

The next important double excitations are $\Phi_2[9a^2 \rightarrow 10a^2]$ ($|\text{CI}|^2 = 0.01$) and $\Phi_3[27a^2 \rightarrow 28a^2]$ ($|\text{CI}|^2 = 0.01$). The energy difference between the 7S and 1S isomers is 82.1 kcal mol⁻¹ (Table 3), which is 24.1 kcal mol⁻¹ higher than the preceding lower-lying structure 6S.

vi. *Transition States and Second-Order Saddle Points* (Figure 6 and Tables S5–S8 in the Supporting Information). The lowest-lying transition state structure TS1 (*C*_{2v} symmetry, Figure 6) was predicted to be 18.1 kcal mol⁻¹ higher in energy than the global minimum 1S. This transition state appears to

connect two mirror images of isomer 3S through a CH₂ rocking motion and has an equivalent electronic configuration. In principle there is no barrier height for this isomerization reaction (3S → TS1 → 3S). The second transition state found on the PES is *C*_{2v} symmetry structure TS2 (Figure 6). This isomer lies 88.3 kcal mol⁻¹ above the global minimum, with electron configuration similar to that of 6S. TS2 seems to connect two mirror images of isomer 7S via a GeGeH bending motion. Two stationary points of Hessian index 2 (second order saddle point), SSP1 and SSP2, were located on the PES. SSP1 lies relatively low in energy at only 22.6 kcal mol⁻¹ above the global minimum 1S. The highest energy stationary point found in this study is SSP2, which has a relative energy of 103.7 kcal mol⁻¹ with respect to our global minimum.

B. Geometries. The predicted geometries of isomers 1S–7S, transition states TS1 and TS2, and second-order saddle points SSP1 and SSP2 optimized at the CCSD(T)/cc-pVQZ level of theory are presented in Figures 2 to 6 and S1–S11 (Supporting Information).

i. *Global Minimum 1S.* The global minimum structure on the Ge₂CH₂ potential energy surface has an unusual cyclic arrangement containing one bridging hydrogen. In this isomer, the Ge–Ge bond distance decreases with advanced treatment of correlation effects to reach 2.674 Å at the highest level of theory as seen in Figure 2 and Figure S1 in the Supporting Information. The reverse trend is observed with the C–Ge distance (1.856 Å) where the bond distance is stretched with increasing correlation level. On the other hand, the Ge–H distance in the bridged Ge...H...Ge connection shows a significant reduction of its length, as the correlation treatment increases, owing it to the delocalized nature of 1S. The Ge–C–Ge angle in this isomer is 92.1°, and the C–Ge–H angle has a magnitude of 84.3°. The Ge–Ge bond distance in the Ge₂H₂ butterfly structure has been found to be 2.39 Å at the CCSD/DZP level of theory,⁶² which is 0.33 Å shorter than in 1S. This indicates a rather weak direct Ge–Ge interaction in the global Ge₂CH₂ minimum. Consequently, the Ge–H bond is also longer for the 1S isomer with higher levels of theory.

ii. *Structure 2S.* The 2S isomer corresponds to the second lowest energy structure and is depicted in Figure 3 and Figure S2 in the Supporting Information. It is another cyclic structure where the hydrogen atom forms only one bond to a germanium atom. The Ge–Ge bond distance shortens relative to 1S by 0.24 Å to 2.430 Å at the CCSD(T)/cc-pVQZ level of theory. There is also a noticeable effect on the bond length upon more sophisticated treatments of correlation, since the Ge1–Ge2 bond length decreases by 0.27 Å when going from the SCF/cc-pVQZ to the CCSD(T)/cc-pVQZ level of theory. A very significant dependence on the level of theory is observed in the Ge–C bond distances. At the SCF level of theory the Ge1–C and Ge2–C bond lengths are 1.917 Å and 1.801 Å, respectively. However when increasing the level of electron correlation treatment, the Ge1–C bond contracts to 1.856 Å and Ge2–C becomes the slightly longer bond with a distance of 1.878 Å. The Ge–C–Ge angle (81.2°) is noticeably smaller compared to the corresponding angle (92.1°) in 1S. In the analogous monobridged Ge₂H₂ structure, one hydrogen is solely bonding to one germanium, while the other hydrogen is bridged between the two germanium atoms.⁶² The Ge–Ge bond distance in this Ge₂H₂ isomer is 2.27 Å (CCSD/DZP), which is again shorter than the 2.43 Å Ge–Ge distance in 2S. However the Ge–H distance is comparable with 1.55 Å for the monobridged Ge₂H₂ structure and 1.53 Å in 2S.

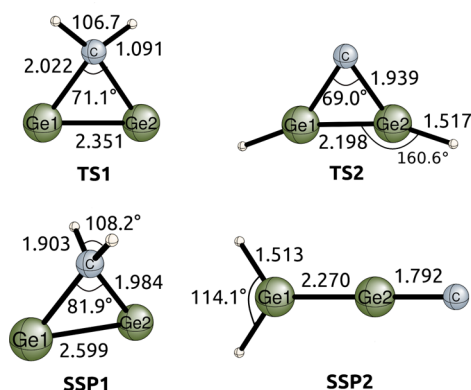


Figure 6. Geometries of the transition states TS1 and TS2 and second-order saddle points SSP1 and SSP2 optimized at the CCSD(T)/cc-pVQZ level of theory.

Table 4. Harmonic Vibrational Frequencies (in cm^{-1}), IR Intensities (in km mol^{-1} in Square Brackets), and Zero-Point Vibrational Energy Correction (ZPVE in kcal mol^{-1}) for the 11 Stationary Points at the CCSD(T) cc-pVQZ Level of Theory

structures	energy	symmetry	ω_1	ω_2	ω_3	ω_4	ω_5	ω_6	ω_7	ω_8	ω_9	ZPVE
1S	−4190.507579	C_{2v}	3250(a_1) [0.6]	1435(a_1) [16.0]	763(a_1) [24.6]	268(a_1) [0.5]	852(b_1) [14.1]	463(b_1) [26.3]	1100(b_2) [304.3]	755(b_2) [5.7]	668(b_2) [9.5]	13.66
2S	−4190.47846	C_s	3202(a') [1.9]	2121(a') [139.8]	837(a') [44.9]	778(a') [23.7]	669(a') [21.8]	374(a') [4.8]	194(a') [29.2]	748(a'') [74.9]	353(a'') [5.8]	13.26
3S	−4190.478052	C_s	3147(a') [7.4]	2763(a') [11.8]	1428(a') [7.8]	647(a') [22.0]	414(a') [4.0]	385(a') [38.1]	236(a') [6.6]	714(a'') [78.5]	259(a'') [0.1]	14.29
4S	−4190.453764	C_{2v}	3135(a_1) [1.4]	1382(a_1) [1.1]	763(a_1) [2.0]	302(a_1) [17.0]	711(b_1) [24.9]	39(b_1) [0.0]	3242(b_2) [0.4]	713(b_2) [0.9]	60(b_2) [2.6]	14.79
5S	−4190.445568	C_{2v}	2227(a_1) [96.0]	1269(a_1) [271.5]	893(a_1) [107.9]	339(a_1) [1.0]	525(b_1) [15.8]	86(b_1) [7.0]	2223(b_2) [80.0]	582(b_2) [53.9]	128(b_2) [15.0]	11.83
6S	−4190.408783	C_{2v}	2044(a_1) [102.2]	630(a_1) [66.6]	374(a_1) [0.5]	116(a_1) [1.2]	527(a_2) [0.0]	124(b_1) [5.6]	2034(b_2) [185.0]	960(b_2) [2.4]	196(b_2) [162.8]	10.02
7S	−4190.369076	C_s	2087(a') [135.9]	2047(a') [94.8]	784(a') [11.9]	644(a') [9.0]	423(a') [11.2]	281(a') [34.0]	178(a') [3.2]	341(a'') [0.7]	156(a'') [5.9]	9.92
TS1	−4190.47741	C_{2v}	3074(a_1) [5.4]	1323(a_1) [13.8]	585(a_1) [28.7]	305(a_1) [0.3]	256(a_2) [0.0]	711(b_1) [85.7]	3122(b_2) [3.8]	415(b_2) [3.9]	213i(b_2) [38.5]	14.0
TS2	−4190.364368	C_{2v}	2170(a_1) [10.7]	737(a_1) [0.7]	517(a_1) [4.8]	354(a_1) [1.2]	337(a_2) [0.0]	342(b_1) [0.0]	2174(b_2) [143.1]	524(b_2) [13.3]	127i(b_2) [18.4]	10.23
SSP1	−4190.467149	C_{2v}	3042(a_1) [0.6]	1282(a_1) [6.4]	617(a_1) [61.3]	223(a_1) [2.6]	304i(a_2) [0.0]	3103(b_1) [0.0]	449i(b_1) [0.1]	803(b_2) [1.8]	460(b_2) [0.0]	13.62
SSP2	−4190.332438	C_{2v}	2225(a_1) [50.0]	847(a_1) [132.4]	831(a_1) [1.0]	288(a_1) [0.4]	300(b_1) [5.7]	62i(b_1) [6.5]	2247(b_2) [37.7]	427(b_2) [16.9]	27i(b_2) [1.3]	10.24

iii. Structure 3S. The 3S cyclic structure is very close in energy to 2S with the difference being only $1.08 \text{ kcal mol}^{-1}$. In this structure the carbon atom has the two hydrogen atoms bound to it, as depicted in Figure 4 and Figure S3 in the Supporting Information. The most remarkable features of 3S are the tetravalent planar carbon and the unusually long C–H bond distance, 1.121 \AA . The Ge1–Ge2 bond distance of 2.379 \AA is 0.05 \AA shorter than in 2S at the CCSD(T)/cc-pVQZ level of theory. On the other hand, both of the Ge–C bond lengths (2.086 \AA and 1.936 \AA) are longer relative to 2S (1.856 \AA and 1.878 \AA). Upon increasing level of correlation treatment, the Ge1–C bond is slightly contracted, whereas the Ge2–C distance increases. The Ge–C–Ge bond angle (72.4°) is 8.8° smaller than the same angle in 2S. The favorability of this rare tetravalent planar carbon structure can most likely be attributed to the delocalized π -electron system over the Ge–C–Ge ring ($9a''$ orbital in Figure 4). The 3S germanium–germanium distance is not consistent with the $\text{Ge}\equiv\text{Ge}$ bond that might be expected for a structure valence isoelectronic with cyclopropyne.²⁵

iv. Structures 4S and 5S. The energetically lowest open chain isomer 4S is shown in Figure 5 and Figure S4 in the Supporting Information. In this germylidene structure the two hydrogen atoms form bonds with carbon. The two germaniums lie on the same axis as carbon, resulting in a C_{2v} symmetric structure. 4S lies $31.7 \text{ kcal mol}^{-1}$ higher in energy than the global minimum. The Ge–Ge bond distance of 2.264 \AA is shorter than in all the aforementioned structures. The H–C–H bond angle is 116.9° . Structure 5S in Figure 5 and Figure S5 in the Supporting Information also has a noncyclic structure. In this isomer the two hydrogen atoms are bound to germanium and the carbon atom is the central part of the Ge–C–Ge backbone. The Ge–C bond lengths are 1.764 \AA and 1.754 \AA . The H–C–H bond angle is only slightly changed with respect to 4S amounting to 112.5° .

v. Structures 6S and 7S (in Figure 5 and Figures S6 and S7 in the Supporting Information). The two highest lying

minimum (equilibrium) structures are the carbene-like isomers 6S and 7S. In 6S (Figure 5 and Figure S6 in the Supporting Information) the Ge–C bond distance is 1.814 \AA , which is comparable to the Ge–C bond length in structures 4S and 5S. The most noteworthy parameter in 6S is the wide Ge–C–Ge angle. A considerable variation is observed with increasing level of correlation treatments. The angle decreases from 172° at the SCF/cc-pVQZ level of theory to 151° at the CCSD(T)/cc-pVQZ level of theory. Finally, the cyclic 7S isomer (Figure 5 and Figure S7 in the Supporting Information) is the highest lying minimum on the singlet PES. The Ge–Ge bond distance of 2.412 \AA is comparable to that in the other cyclic structures 2S and 3S. However, the C–Ge1 bond (1.810 \AA) is noticeably shorter than the C–Ge2 (2.100 \AA), which is the largest difference between lengths of the Ge–C bond distances among the cyclic isomers.

vi. TS1 and TS2. Structure TS1 (Figure 6 and Figure S8 in the Supporting Information) is a C_{2v} symmetry transition state with one imaginary vibrational frequency corresponding to the CH_2 rocking motion. This normal mode connects the two mirror images of the 3S isomer. For this reason the structural features of TS1 and dependence on correlation treatment of geometrical parameters resemble those of 3S. The second transition state found on this PES is the C_{2v} TS2 structure (Figure 6 and Figure S9 in the Supporting Information). This transition state connects two identical 7S isomers, through a HGeGeH bending motion. A noteworthy difference between TS2 and 7S is the different lengths of the Ge–Ge bond. The Ge–Ge bond distance of 2.198 \AA in TS2 is the shortest Ge–Ge bond among all stationary points located in this study. This is consistent with a $\text{Ge}=\text{Ge}$ double bond that one would associate with the valence isoelectronic cyclopropenyldiene.

vii. SSP1 and SSP2. Lastly, two stationary points of Hessian index 2 were found on the singlet PES. The lower in energy is the cyclic SSP1 (Figure 6 and Figure S10 in the Supporting Information), and it is the only nonplanar stationary point. The Ge–Ge bond (2.599 \AA) is quite elongated, second only to the

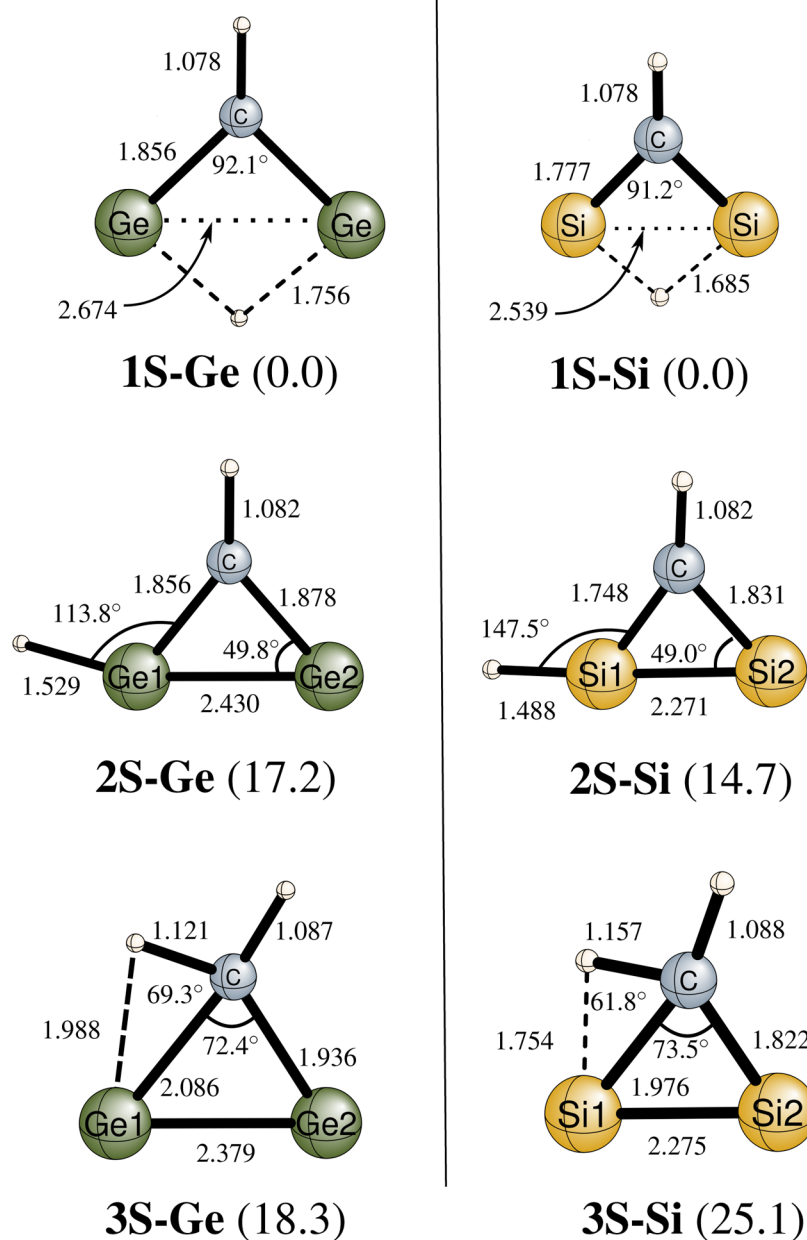


Figure 7. Structure and energy comparison of the three lowest lying isomers in the Ge_2CH_2 and Si_2CH_2 PES. The energies and structural parameters for Si_2CH_2 are taken from Wu et al.³¹ (CCSDT CBS/CCSD(T) cc-pVQZ level of theory). The energies for Ge_2CH_2 are ΔE_{final} . Bond lengths are in Å and energies in parentheses in kcal mol^{-1} .

global minimum **1S**, thus suggesting a rather weak Ge–Ge single bond. This bond distance decreases with increasing level of correlation, following the trend observed for the other cyclic isomers. The **SSP2** structure (Figure 6 and Figure S11 in the Supporting Information) is the highest lying stationary point found in this study. It is a noncyclic vinylidene structure with a terminal carbon and both germanium atoms on the C_2 symmetry axis.

C. Harmonic Vibrational Frequencies. The nature of the stationary points has been characterized through harmonic vibrational frequency analysis. Seven minima, two transition states, and two second order saddle points were identified among the 11 stationary points considered in this study. The harmonic vibrational frequencies (in wavenumbers) of the nine normal modes together with ZPVE values at the CCSD(T) cc-pVQZ level of theory are given in Table 4. The harmonic

vibrational frequencies for other levels of theory may be found in the Supporting Information. The stationary points **1S** through **7S** were found to have all real frequencies at every level of theory. The only exception is **7S**, which is a transition state at the SCF level of theory, and once correlation effects are added it becomes a minimum on the PES. The imaginary frequency of **TS1** corresponds to a rocking motion of the CH_2 group. Finally, the two imaginary frequencies detected for the second order saddle point **SSP1** correspond to an out of plane rocking motion and a twisting motion of the CH_2 group. For **SSP2** the two imaginary frequencies may be assigned to an out-of plane and an in-plane bending Ge–Ge–C motion.

D. Comparison to Si_2CH_2 . As it is the case for the X_2H_2 ($\text{X} = \text{Si}, \text{Ge}$) system, the low energy structures of X_2CH_2 are qualitatively similar. The three energetically lowest isomers correspond to cyclic structures and are shown in Figure 7. The

global minimum for both systems incorporates a bridging hydrogen atom. Besides the difference in X–C and X–X bond lengths due to the unequal size of silicon and germanium atoms, the two hydrogen bridged isomers are structurally very similar. This can be seen by comparing the X–C–X angle, which is around 92° in both the **1S-Si** and **1S-Ge**. The value of the inner ring angles for the second lowest isomers **2S-Si** and **2S-Ge** are similar as well. The most striking difference in these structures is the H–X–C angle, which is 147.5° in **2S-Si** and decreases to 113.8° in **2S-Ge**. The energy of **2S-Si** is $14.7 \text{ kcal mol}^{-1}$ higher in energy than the global minimum, whereas the same structure in Ge_2CH_2 is located $17.2 \text{ kcal mol}^{-1}$ higher than **1S-Ge**. In **3S-Ge**, as it was the case in **1S-Ge** and **2S-Ge**, the X–C–X angle of the silicon and germanium structures differs only by one degree. On the other hand the H–C–X angle increases from 61.8° to 69.3° , indicating a weaker H–Ge than H–Si interaction. Furthermore, the C–H distance of **3S-Si** is noticeably longer (1.157 \AA) than in **3S-Ge** (1.121 \AA). This is another indication for a stronger bridging character in the silicon structure. However the energy with respect to the global minimum in **3S-Ge** amounts to $18.3 \text{ kcal mol}^{-1}$, which is $6.8 \text{ kcal mol}^{-1}$ lower than **3S-Si**. Therefore, the larger bridging character of the hydrogen in **3S-Si** does not seem to bear a significant stabilizing influence on the relative energies of the **3S-Ge** and **3S-Si** structures. The largest energetic difference between the Si_2CH_2 and Ge_2CH_2 PES can be found in the linear C_{2v} structures. In Si_2CH_2 the structure with the central carbon lies at $28.1 \text{ kcal mol}^{-1}$, while the isomer with terminal methylene is located $45.0 \text{ kcal mol}^{-1}$ above the global minimum.³¹ Notwithstanding, in Ge_2CH_2 the energy ordering of these two structures is inverted such that the isomer with the terminal methylene lies at $31.7 \text{ kcal mol}^{-1}$ and the structure with the central carbon is located $8.2 \text{ kcal mol}^{-1}$ higher. A possible explanation may be the different π -bond energies of C–Si, C–Ge, Ge–Ge, and Si–Si bonds.⁶³ Finally in both potential energy surfaces, the carbene structures lie highest in energy.

IV. CONCLUDING REMARKS

Through the use of state-of-the-art *ab initio* electronic structure theory, the lowest singlet potential energy structure of Ge_2CH_2 was systematically investigated. Eleven stationary points are found among which there are seven minima, two transition states, and two second order saddle points. After focal point analysis and adding ZPVE, DBOC, core and relativistic corrections, the energy ordering of the seven minima is predicted to be **1S** [0.0] < **2S** [17.2] < **3S** [18.3] < **4S** [31.7] < **5S** [39.9] < **6S** [58.1] < **7S** [82.1]. The findings concerning the electronic structure of the seven minima indicate the following:

1. Using the kick^{35–37} procedure it was possible to systematically explore the PES of Ge_2CH_2 for unconventional structures.
2. Cyclic arrangements found in **1S**, **2S**, and **3S** are the energetically most favorable structures for the Ge_2CH_2 system.
3. An isomer incorporating a rare tetravalent planar carbon (**3S**) is found among the low energy minima, and its relative energy is lower than the analogous structure in the Si_2CH_2 PES.
4. The carbene-like structures (**6S** and **7S**) are the least favored on the Ge_2CH_2 PES.

We hope that our predictions will encourage future experimental investigations on these novel digermanium compounds.

■ ASSOCIATED CONTENT

Supporting Information

Focal point tables for structures **4S** through **SSP2**. Harmonic vibrational frequencies and theoretical structures for the SCF-RHF, CCSD, CCSD(T) methods, with cc-pVDZ, cc-pVTZ and cc-pVQZ basis sets. This material is available free of charge via the Internet at <http://pubs.acs.org>.

■ AUTHOR INFORMATION

Corresponding Author

*E-mail: qc@uga.edu.

Notes

The authors declare no competing financial interest.

■ ACKNOWLEDGMENTS

This research was supported by the U.S. National Science Foundation Grant CHE-1054286.

■ REFERENCES

- (1) Tsumuraya, T.; Batcheller, S.; Masamune, S. Strained-Ring and Double-Bond Systems Consisting of the Group-14 Elements Si, Ge, and Sn. *Angew. Chem., Int. Ed.* **1991**, *30*, 902–930.
- (2) Driess, M.; Grutzmacher, H. Main Group Element Analogues of Carbenes, Olefins, and Small Rings. *Angew. Chem., Int. Ed.* **1996**, *35*, 829–856.
- (3) Power, P. P. π -Bonding and the Lone Pair Effect in Multiple Bonds between Heavier Main Group Elements. *Chem. Rev.* **1999**, *99*, 3463–3504.
- (4) Sekiguchi, A.; Tsukamoto, M.; Ichinohe, M. A Free Cyclo-trigermanium Cation with a 2π -Electron System. *Science* **1997**, *275*, 60–61.
- (5) Schleyer, P. v. R. Germanyl and Silyl Cations: Free at Last. *Science* **1997**, *275*, 39–40.
- (6) Lee, V. Y.; Sekiguchi, A. Aromaticity of Group 14 Organometallics: Experimental Aspects. *Angew. Chem., Int. Ed.* **2007**, *46*, 6596–6620.
- (7) Lee, V. Y.; Sekiguchi, A. Stable Silyl, Germyl, and Stannyl Cations, Radicals, and Anions: Heavy Versions of Carbocations, Carbon Radicals, and Carbanions. *Acc. Chem. Res.* **2007**, *40*, 410–419.
- (8) Mizuhata, Y.; Sasamori, T.; Tokitoh, N. Stable Heavier Carbene Analogues. *Chem. Rev.* **2009**, *109*, 3479–3511.
- (9) Lavallo, V.; Canac, Y.; Donnadiou, B.; Schoeller, W. W.; Bertrand, G. Cyclopropenylidenes: From Interstellar Space to an Isolated Derivative in the Laboratory. *Science* **2006**, *312*, 722–4.
- (10) Mandal, S. K.; Roesky, H. W. Interstellar Molecules: Guides for New Chemistry. *Chem. Commun.* **2010**, *46*, 6016–6041.
- (11) Reisenauer, H. P.; Maier, G.; Riemann, A.; Hoffmann, R. W. Cyclopropenylidene. *Angew. Chem., Int. Ed.* **1984**, *23*, 641–641.
- (12) Seburg, R. A.; Patterson, E. V.; Stanton, J. F.; McMahon, R. J. Structures, Automerizations, and Isomerizations of C_3H_2 Isomers. *J. Am. Chem. Soc.* **1997**, *119*, 5847–5856.
- (13) Seburg, R. A.; McMahon, R. J. Automerizations and Isomerizations in Propynylidene (HCCCCH), Propadienylidene (H_2CCC), and Cyclopropenylidene ($\text{c-C}_3\text{H}_2$). *Angew. Chem., Int. Ed.* **1995**, *34*, 2009–2012.
- (14) Achkassova, E.; Araki, M.; Denisov, A.; Maier, J. P. Gas Phase Electronic Spectrum of Propadienylidene C_3H_2 . *J. Mol. Spectrosc.* **2006**, *237*, 70–75.
- (15) Hemberger, P.; Noller, B.; Steinbauer, M.; Fischer, K.; Fischer, I. The $\text{B } ^1\text{B}_1$ State of Cyclopropenylidene, $\text{c-C}_3\text{H}_2$. *J. Phys. Chem. Lett.* **2010**, *1*, 228–231.

- (16) Lee, T. J.; Bunge, A.; Schaefer, H. F., III Toward the Laboratory Identification of Cyclopropenylidene. *J. Am. Chem. Soc.* **1985**, *107*, 137–142.
- (17) Rubio, M.; Stålring, J.; Bernhardsson, A.; Lindh, R.; Roos, B. O. Theoretical Studies of Isomers of C_3H_2 Using a Multiconfigurational Approach. *Theor. Chem. Acc.* **2000**, *105*, 15–30.
- (18) Lee, T. J.; Huang, X.; Dateo, C. E. The Effect of Approximating Some Molecular Integrals in Coupled-Cluster Calculations: Fundamental Frequencies and Rovibrational Spectroscopic Constants for Isotopologues of Cyclopropenylidene. *Mol. Phys.* **2009**, *107*, 1139–1152.
- (19) Wu, Q.; Cheng, Q.; Yamaguchi, Y.; Li, Q.; Schaefer, H. F., III Triplet States of Cyclopropenylidene and Its Isomers. *J. Chem. Phys.* **2010**, *132*, 044308.
- (20) Frenking, G.; Remington, R. B.; Schaefer, H. F. Structures and Energies of Singlet Silacyclopropenylidene and 14 Higher Lying C_2SiH_2 Isomers. *J. Am. Chem. Soc.* **1986**, *108*, 2169–2173.
- (21) Maier, G.; Reisenauer, H. P.; Pacl, H. C_2H_2Si Isomers: Generation by Pulsed Flash Pyrolysis and Matrix-Spectroscopic Identification. *Angew. Chem., Int. Ed.* **1994**, *33*, 1248–1250.
- (22) Maier, G.; Pacl, H.; Reisenauer, H. P.; Meudt, A.; Janoschek, R. Silacyclopropyne: Matrix Spectroscopic Identification and *ab initio* Investigations. *J. Am. Chem. Soc.* **1995**, *117*, 12712–12720.
- (23) Maier, G.; Reisenauer, H.; Egenolf, H. Hetero π systems. Reaction of Silicon Atoms With Acetylene and Ethylene: Generation and Matrix-Spectroscopic Identification of C_2H_2Si and C_2H_4Si Isomers. *Eur. J. Org. Chem.* **1998**, 1313–1317.
- (24) Vacek, G.; Colegrove, B. T.; Schaefer, H. F., III The Infrared Spectrum of Silacyclopropenylidene. *J. Am. Chem. Soc.* **1991**, *113*, 3192–3193.
- (25) Sherrill, C. D.; Brandow, C. G.; Allen, W. D.; Schaefer, H. F., III Cyclopropyne and Silacyclopropyne: A World of Difference. *J. Am. Chem. Soc.* **1996**, *118*, 7158–7163.
- (26) Ikuta, S.; Saitoh, T.; Wakamatsu, S. Theoretical Study on Isomeric Stabilities of C_2H_2Si and Its Ionization Potentials and Electron Affinities. *J. Chem. Phys.* **2004**, *121*, 3478–85.
- (27) Thorwirth, S.; Harding, M. E. Coupled-Cluster Calculations of C_2H_2Si and $CNHSi$ Structural Isomers. *J. Chem. Phys.* **2009**, *130*, 214303.
- (28) Wu, Q.; Simmonett, A. C.; Yamaguchi, Y.; Li, Q.; Schaefer, H. F., III Silacyclopropenylidene and Its Most Important SiC_2H_2 Isomers. *J. Phys. Chem. C* **2010**, *114*, 5447–5457.
- (29) Jemmis, E. D.; Prasad, B. V.; Tsuzuki, S.; Tanabe, K. Analogy Between Trivalent Boron and Divalent Silicon. *J. Phys. Chem.* **1990**, *94*, 5530–5535.
- (30) Ikuta, S.; Wakamatsu, S. *Ab Initio* Molecular Orbital Study of Structures and Energetics of Si_3H_2 , $Si_3H_2^+$, and $Si_3H_2^-$. *J. Chem. Phys.* **2004**, *120*, 11071–81.
- (31) Wu, Q.; Hao, Q.; Yamaguchi, Y.; Li, Q.; Fang, D.-C.; Schaefer, H. F., III Unusual Isomers of Disilacyclopropenylidene (Si_2CH_2). *J. Phys. Chem. A* **2010**, *114*, 7102–7109.
- (32) Lu, T.; Wilke, J. J.; Yamaguchi, Y.; Schaefer, H. F. Anharmonic Rovibrational Analysis for Disilacyclopropenylidene (Si_2CH_2). *J. Chem. Phys.* **2011**, *134*, 164101–164107.
- (33) Teng, Y.-L.; Xu, Q. Reactions of Group 14 Metal Atoms with Acetylene: A Matrix Isolation Infrared Spectroscopic and Theoretical Study. *J. Phys. Chem. A* **2009**, *113*, 12163–12170.
- (34) Hao, Q.; Simmonett, A. C.; Yamaguchi, Y.; Fang, D.-C.; Schaefer, H. F., III From Acetylene Complexes to Vinylidene Structures: The GeC_2H_2 system. *J. Comput. Chem.* **2011**, *32*, 15–22.
- (35) Saunders, M. Stochastic Search for Isomers on a Quantum Mechanical Surface. *J. Comput. Chem.* **2004**, *25*, 621–624.
- (36) Bera, P. P.; Sattelmeyer, K. W.; Saunders, M.; Schaefer, H. F., III; Schleyer, P. v. R. Mindless Chemistry. *J. Phys. Chem. A* **2006**, *110*, 4287–4290.
- (37) Wheeler, S. E.; Schleyer, P. v. R.; Schaefer, H. F. SASS: A Symmetry Adapted Stochastic Search Algorithm Exploiting Site Symmetry. *J. Chem. Phys.* **2007**, *126*, 104104.
- (38) Shao, Y.; et al. Advances in Methods and Algorithms in a Modern Quantum Chemistry Program Package. *Phys. Chem. Chem. Phys.* **2006**, *8*, 3172–3191.
- (39) Thom H. Dunning, J. Gaussian Basis Sets for Use in Correlated Molecular Calculations. I. The Atoms Boron Through Neon And Hydrogen. *J. Chem. Phys.* **1989**, *90*, 1007–1023.
- (40) Rittby, M.; Bartlett, R. J. An Open-Shell Spin-Restricted Coupled Cluster Method: Application to Ionization Potentials in Nitrogen. *J. Phys. Chem.* **1988**, *92*, 3033–3036.
- (41) Purvis, G. D.; Bartlett, R. J. A Full Coupled-Cluster Singles and Doubles Model: The Inclusion of Disconnected Triples. *J. Chem. Phys.* **1982**, *76*, 1910–1918.
- (42) Raghavachari, K.; Trucks, G. W.; Pople, J. A.; Head-Gordon, M. A Fifth-Order Perturbation Comparison of Electron Correlation Theories. *Chem. Phys. Lett.* **1989**, *157*, 479–483.
- (43) Stanton, J. F. Why CCSD(T) Works: A Different Perspective. *Chem. Phys. Lett.* **1997**, *281*, 130–134.
- (44) Watts, J. D.; Gauss, J.; Bartlett, R. J. Open-Shell Analytical Energy Gradients for Triple Excitation Many-Body, Coupled-Cluster Methods: MBPT(4), CCSD+T(CCSD), CCSD(T), and QCISD(T). *Chem. Phys. Lett.* **1992**, *200*, 1–7.
- (45) Kallay, M.; Surjan, P. R. Higher Excitations in Coupled-Cluster Theory. *J. Chem. Phys.* **2001**, *115*, 2945–2954.
- (46) Kallay, M.; Gauss, J. Approximate Treatment of Higher Excitations in Coupled-Cluster Theory. *J. Chem. Phys.* **2005**, *123*, 214105.
- (47) Claude A. Richards, J.; Yamaguchi, Y.; Kim, S.-J.; S., H. F., III The GaOH–HGao Potential Energy Hypersurface and the Necessity of Correlating the 3d Electrons. *J. Chem. Phys.* **1996**, *104*, 8516–8523.
- (48) Siegbahn, P.; Heiberg, A.; Roos, B.; Levy, B. A Comparison of the Super-CI and the Newton-Raphson Scheme in the Complete Active Space SCF Method. *Phys. Scr.* **1980**, *21*, 323–327.
- (49) Roos, B.; Taylor, P.; Siegbahn, P. E. M. A Complete Active Space SCF Method (CASSCF) Using a Density Matrix Formulated Super-CI Approach. *Chem. Phys.* **1980**, *48*, 157–173.
- (50) Löwdin, P.-O.; Shull, H. Natural Orbitals in the Quantum Theory of Two-Electron Systems. *Phys. Rev.* **1956**, *101*, 1730–1739.
- (51) Császár, A. G.; Allen, W. D.; Schaefer, H. F., III In Pursuit of the *ab Initio* Limit for Conformational Energy Prototypes. *J. Chem. Phys.* **1998**, *108*, 9751–9764.
- (52) Schuurman, M. S.; Muir, S. R.; Allen, W. D.; Schaefer, H. F., III Toward Subchemical Accuracy in Computational Thermochemistry: Focal Point Analysis of the Heat of Formation of NCO and $[H,N,C,O]$ Isomers. *J. Chem. Phys.* **2004**, *120*, 11586–11599.
- (53) Gonzales, J. M.; Pak, C.; Cox, R. S.; Allen, W. D.; Schaefer, H. F., III; Császár, A. G.; Tarczay, G. Definitive *ab Initio* Studies of Model S_N2 Reactions $CH_3X + F^-$ ($X = F, Cl, CN, OH, SH, NH_2, PH_2$). *Chem.—Eur. J.* **2003**, *9*, 2173–2192.
- (54) Császár, A. G.; Tarczay, G.; Leininger, M. L.; Polyansky, O. L.; Tennyson, J.; Allen, W. D. In *Spectroscopy from Space*; Demaison, J., Sarka, K., Eds.; Kluwer: Dordrecht, 2001; pp 317–340.
- (55) Helgaker, T.; Klopper, W.; Koch, H.; Noga, J. Basis Set Convergence of Correlated Calculations on Water. *J. Chem. Phys.* **1997**, *106*, 9639–9646.
- (56) Feller, D. The Use of Systematic Sequences of Wave Functions for Estimating the Complete Basis Set, Full Configuration Interaction Limit in Water. *J. Chem. Phys.* **1993**, *98*, 7059–7071.
- (57) Werner, H.-J.; Knowles, P. J.; Knizia, G.; Manby, F. R.; Schütz, M.; et al.; MOLPRO, Version 2012.1, a Package of *ab Initio* Programs; 2012.
- (58) Gauss, J.; Tajti, A.; Kallay, M.; Stanton, J. F.; Szalay, P. G. Analytic Calculation of the Diagonal Born-Oppenheimer Correction Within Configuration-Interaction and Coupled-Cluster Theory. *J. Chem. Phys.* **2006**, *125*, 144111–144121.
- (59) Michauk, C.; Gauss, J. Perturbative Treatment of Scalar-Relativistic Effects in Coupled-Cluster Calculations of Equilibrium Geometries and Harmonic Vibrational Frequencies Using Analytic Second-Derivative Techniques. *J. Chem. Phys.* **2007**, *127*, 044106.

- (60) Stanton, J.; Gauss, J.; Watts, J.; Szalay, P.; Bartlett, R.; et al.; *CFOUR, a Quantum Chemical Program Package*; 2009.
- (61) Lide, D. R.; Bruno, T. J. *CRC Handbook of Chemistry and Physics*; CRC Press LLC: 2012.
- (62) Palagyi, Z.; Schaefer, H. F., III; Kapuy, E. Ge_2H_2 : A Germanium Containing Molecule with a Low-Lying Monobridged Equilibrium Geometry. *J. Am. Chem. Soc.* **1993**, *115*, 6901–6903.
- (63) Windus, T. L.; Gordon, M. S. π -Bond Strengths of $\text{H}_2\text{X}:\text{YH}_2$: X = Ge, Sn; Y = C, Si, Ge, Sn. *J. Am. Chem. Soc.* **1992**, *114*, 9559–9568.